

# High on/off ratio ns laser pulses for a triggered single-photon source

Gang Jin<sup>1, 2</sup>, Bei Liu<sup>1, 2</sup>, Jun He<sup>1, 2, 3</sup>, and Junmin Wang<sup>1, 2, 3,\*</sup>

1). State Key Laboratory of Quantum Optics and Quantum Optics Devices (Shanxi University),

2). Institute of Opto-Electronics, Shanxi University,

3). Collaborative Innovation Center of Extreme Optics (Shanxi University),

No.92 Wu Cheng Road, Tai Yuan 030006, Shan Xi Province, People's Republic of China

**Abstract:** 852nm nano-second laser pulse chain with a high on/off ratio is generated via chopping a continuous-wave laser beam by using of a Mach-Zehnder-type electro-optic intensity modulator (MZ-EOIM). Detailed analysis and dependence of the on/off ratio on the splitting ratio, the co-splitting ratio, and the arms loss of MZ-EOIM are presented. By optimizing the polarization of incident laser beam and stabilizing MZ-EOIM temperature, the static on/off ratio of 12600:1 is achieved. Also the dynamic on/off ratios versus the pulse repetition rate and the pulse duty cycle are measured and discussed. This high on/off ratio ns pulsed laser system has served as the excitation pulse source for a triggered single-photon source based on trapped single cesium atom, which reveals a representative anti-bunching.

**Keywords:** Electro-optic intensity modulator, Nano-second laser pulse, High on/off ratio, Temperature stabilization.

**PACS number(s):** 42.30.Lr, 42.81.Qb, 42.82.Gw, 42.65.Re.

## I. INTRODUCTION

Integrated optical devices play important roles in the fields of high-speed fiber telecom and laser technology due to advances in flexibility, small size, high sensitivity and other characteristics. LiNbO<sub>3</sub> optical waveguide devices can ultrafast modulate laser's amplitude, phase, and frequency [1, 2]. For LiNbO<sub>3</sub> waveguide Mach-Zehnder-type electro-optic intensity modulator (MZ-EOIM), square-wave electrical pulses applied on the modulation port can slice a continuous-wave laser beam into a rectangle wave with typical pulse duration on order of nanosecond even less, which could serve as excitation light to implement a triggered single-photon source [3-5]. In order to achieve a nearly deterministic triggered single-photon source, it requires realizing a high on/off ratio excitation laser pulses. However, due to the limited fabrication technology [6] in the manufacture process of MZ-EOIM, polarization fluctuations of incident laser and thermal drift may cause a significant fluctuation of output pulses at minimum intensity, which is defined as OFF state, the maximum transmission is defined as ON state.

As shown in Fig.1, after initially prepared single Cs atom trapped in a microscopic optical tweezer [7] in the ground Zeeman state  $|F_g=4, m_F=+4\rangle$ . Applied by a resonant  $\sigma^+$ -polarized  $\pi$  pulse (pulse duration  $t_e = 5$  ns), the atom can be excited to  $6P_{3/2} |F_e=5, m_F=+5\rangle$ . The spontaneously emitted photons can be collected by a high numerical aperture lens assembly, Moreover, to reduce the multiphoton events in the single-photon source, the laser intensity of OFF state should closer to zero to avoid the atom being excited by the residual photons. Therefore increasing the ratio of maximum and minimum power (on/off ratio) of the output pulsed light is particularly important.

---

\* Corresponding author: [wwjjmm@sxu.edu.cn](mailto:wwjjmm@sxu.edu.cn)

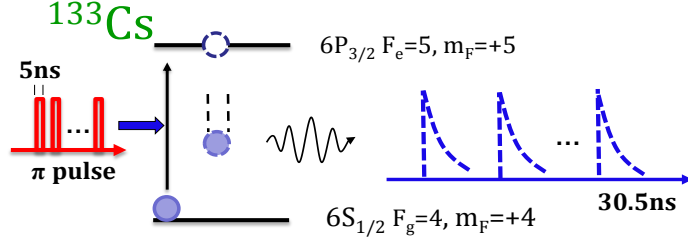


**Fig. 1.** (Color online) Schematic diagram of single photon source based on periodic excitation of a trapped single cesium atom.

Generally, the on/off ratio of commercial MZ-EOIM at wavelength of 850nm not as good as for 1550nm devices, two questions need to solve in the pulse train generated by MZ-EOIM, one is the reducing the power at OFF state as low as possible, and another is stabilize the power of OFF state. The on/off ratio of output pulsed light depends on the symmetry of the two arms of MZ interferometer, the temperature, the polarization of input laser, and the external stress [6]. The DC bias voltage at the OFF point drifts over time, resulting in the fluctuation of output power of ON and OFF state. There are possible approaches to improve the stability and increase on/off ratio of MZ-EOIM. One is optimizing the structure of the modulator design [8, 9]. Specially designed Y-type coupler and waveguide dimensions can decrease insert losses and improve the symmetry of the structure, where the MZ-EOIM polarization and power fluctuation can be decreased. However, this approach has high demands for technical accuracy and fabrication to coincide with theoretical calculation. By searching for the proper DC bias voltage of the OFF state using the external modulation way, Dingjan et al. [5], Snoddy et al. [10], and Bui et al. [11] implemented negative feedback in real-time to re-calibrate DC operating point. But this approach would bring extra unwanted intensity fluctuation, due to the modulation signal used for the feedback loop around the MZ-EOIM. For the double or more MZ-EOIMs in series, the overall transmitted light on/off ratio of two MZ-EOIMs is the product of the two on/off ratio in principle, but the limited input power of and insertion loss of cascade MZ-EOIMs [2, 12] result in a lower output power. Moreover, before using in the high-frequency signal applications, it is difficult to keep synchronization in time when the electric signal applied to two modulators. In this letter, by finely matching the polarization of input light using single-mode polarization maintaining (PM) fiber and precisely stabilizing temperature, the modulator is free sensitivity of the temperature [13] and polarization [14] fluctuation. It is significant that the output laser on/off ratio can also be increased.

The rest of this paper is organized as follows. In Sec. II we introduce detailed analysis and dependence of the on/off ratio on the splitting ratio, the co-splitting ratio, and the arms loss of MZ-EOIM. In Sec. III we develop pulse generation system and active temperature stabilization of MZ-EOIM. In Sec. IV we measured and analyzed the dependence of optical transfer functions, on/off ratio and power stability in OFF state. Finally, we demonstrate the practicality in triggered single photon source based on single atom in an optical trap. Lastly, we draw our concluding remarks in Sec. V.

## II. PRINCIPLE

Lithium niobate (LiNbO<sub>3</sub>) is used for electrical control the optical phase in each arm of MZ-EOIM,

due to its linear electro-optic effect [15]. According to the principle of MZ interferometer, when the two branches are combined at Y junction, the laser intensity can be changed as shown in Fig. 2. We assume that the incident light wave  $E_0$  is divided into two parts by a ratio  $a^2/(1-a^2)$  at the first Y junction beam splitter, two expected waves propagated in each arm were changed the phase of  $\Delta\phi_1$  and  $\Delta\phi_2$  by the applied electric field. In addition to the different insertion losses, corresponding to two arms transmissivities  $T_1$  and  $T_2$ , respectively. When two beams are combined at the second Y junction by intensity ratio of  $b^2/(1-b^2)$ , the output E can be written as:

$$E = bT_1aE_0 \exp(-i\Delta\phi_1) + \sqrt{1-b^2}T_2\sqrt{1-a^2}E_0 \exp(-i\Delta\phi_2) \quad (1)$$

In the ideal case, the symmetric arms in the MZ-EOIM can be described by  $a^2=1/2$ ,  $b^2=1/2$ ,  $T_1=T_2$ . The output E can be obtained as below:

$$E = \frac{1}{2}T_1E_0 \exp[-i(\Delta\phi_1 + \Delta\phi_2/2)] [\exp(i\Delta\phi/2) + \exp(-i\Delta\phi/2)], \quad (2)$$

Here the phase difference between two arms is  $\Delta\phi = \Delta\phi_2 - \Delta\phi_1$ , the output laser intensity is given by:

$$I \propto |E|^2 = \frac{1}{2}(T_1 E_0)^2 [1 + \cos(\Delta\phi)]. \quad (3)$$

Obviously, the output laser intensity varies with phase difference  $\Delta\phi$ , which is induced by DC-bias voltage  $V_{DC}$ , RF voltage  $V_{RF}(t)$  or temperature. The light waves in the second junction cannot propagate through the waveguide for the opposite phase  $\Delta\phi(t) = \alpha V_{DC} + \beta V_{RF}(t) = (2n+1)\pi$ , here  $n$  is integer,  $\alpha$  and  $\beta$  are  $\pi/3.4V$  and  $\pi/1.7V$ , respectively. The modulator can be turned OFF and ON by suffering the voltage  $V_{RF}(t)$ . Moreover, the reversal speed from the OFF state to the ON state not only depends on the response speed of modulator, but also relates to RF electrical pulse time domain profile. The electrical pulses and laser pulses are measured and shown in Fig. 3, corresponding to pulse width of 1 ns, 2 ns, 3 ns, 4 ns, and 5 ns, respectively. The electrical pulses are provided by a fast pulse generator (AVTech, Model AVM-1-C), laser pulses are achieved from a MZ-EOIM (Eospace, Model AZ-OK5-10- PFA-PFA-850-UL) driven by the electrical pulse under the condition of the DC voltage at OFF state. The laser pulses are detected using a fast photo-detector (New Focus, Model 1554-B, bandwidth: DC~12 GHz, rising time:  $\sim 30$  ps) and recorded by an oscilloscope (Agilent, Model DSO-90254A, bandwidth 2.5 GHz). We could see that the laser pulses' profile coincided with the waveform of the electrical pulses, just the falling edge of the laser pulse is a little bit slower. This caused by the transient process of capacitance between internal electrodes in MZ-EOIM waveguide.

In fact, the degradation of on/off ratio is caused by imbalance of two arms in EOIM. Here we only consider the splitting ratio effected on the results. Assuming  $b^2=1/2$ ,  $T_1=T_2=1$ , the output light intensity in Eq. (1) can be rewritten as following:

$$I \propto |E|^2 = E_0^2 \left[ 1 + 2a\sqrt{1-a^2} \cos(\Delta\phi) \right] / 2. \quad (4)$$

According to Eq. (4), the minimum intensity is no longer zero when  $\Delta\phi = \pi$ , thus on/off ratio R is a finite value:

$$R = \frac{P_{\max}}{P_{\min}} = \frac{1 + 2a\sqrt{1-a^2}}{1 - 2a\sqrt{1-a^2}}. \quad (5)$$

The dependence of theoretical on/off ratio value can be seen in Fig. 4. When the splitting ratio is 50/50, the on/off should be infinite in theory, and it will sharply fall from infinity to below 2000 when the splitting ratio is worse than 52/48. Considering the different losses and the splitting ratio between two arms, the on/off ratio will be no more than 1000 actually. So it is need to conduct an efficient way

to optimize the on/off ratio.

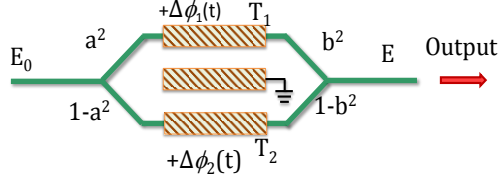


**Fig. 2.** Schematic diagram of MZ- EOIM.

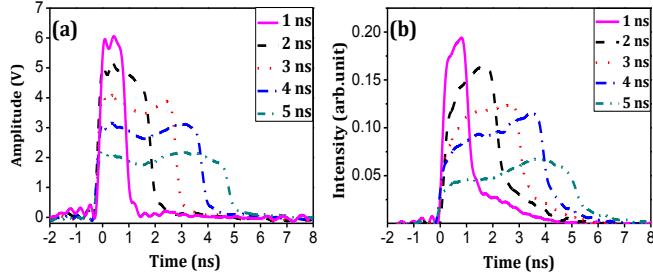


**Fig. 3.** (Color online) (a)The electrical pulses applied to MZ-EOIM and (b) the output laser pulses with different pulse duration

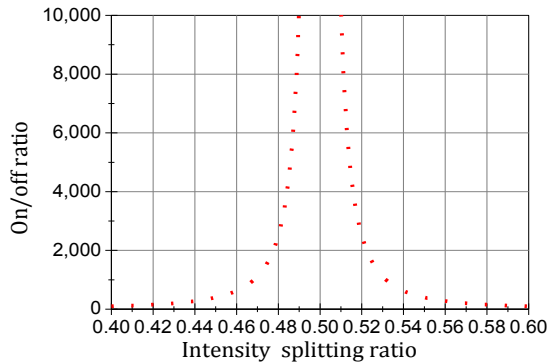


**Fig. 4.** (Color online) Simulation result of the on/off ratio versus the intensity splitting ratio of MZ-EIOM.

### III. EXPERIMENTAL

An extended-cavity diode laser (ECDL, Toptica, Model DL100) provides 852 nm output with the maximum power of 80 mW. As shown in Fig. 5, when the laser frequency is scanned across Cs  $6S_{1/2}$  ( $F_g = 4$ ) -  $6P_{3/2}$  ( $F_e = 3, 4, 5$ ) hyperfine transitions, the corresponding polarization spectra <sup>[15]</sup> can be obtained. We lock the ECDL's frequency to the  $6S_{1/2}$  ( $F_g = 4$ ) -  $6P_{3/2}$  ( $F_e = 5$ ) closed transition by using of the polarization spectra via a proportion-integration (PI) amplifier and the PZT driver of the ECDL.

The main output beam passes through two acousto-optical frequency shifters (AOM1 and AOM2) and the MZ-EOIM, which is inserted between two AOMs to generate high on/off ratio laser pulses for atomic excitation. Here two AOMs are used to change the excitation laser pulses' frequency to match the AC-Stark shifted Cs  $6S_{1/2}$   $|F_g=4, m_F=+4\rangle$  -  $6P_{3/2}$   $|F_e=5, m_F=+5\rangle$  closed transition of trapped single atom in our microscopic optical tweezer <sup>[6]</sup>. Two fiber couplers (FCs) are used to couple the laser beam into (and out from) the MZ-EIOM's input (and output) PM fiber. Before being fed into the MZ-ZOIM via the input PM fiber, the incident beam should be purely linearly-polarized with a high

extinction ratio ( $> 40$  dB). We carefully adjust the incident beam's polarization to match the input PM fiber. The typical transmissivity ( $P_{\text{out}}/P_{\text{in}}$ ) is up to 32% due to the insertion loss. The MZ-EOIM is driven by RF signal (applied to the RF port) with the half-wave voltage  $V_{\pi}$  (typical half-wave voltage is  $V_{\pi} = 3.4$  V). When a DC bias voltage (applied to the bias port) fixed at a minimum transmissivity, the MZ-EOIM produces laser pulse chain periodically changed from the OFF state to the ON state. According to Eq. (3), if the DC bias voltage is changed linearly,  $P_{\text{out}}$  will change as a cosine trend.

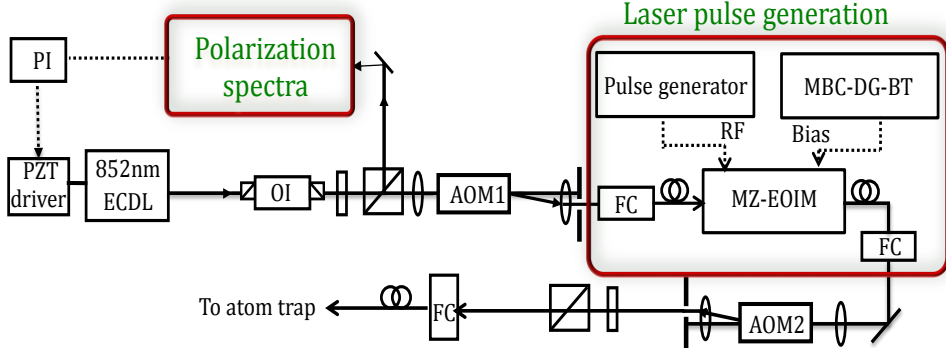


**Fig. 5.** (Color online) Schematic diagram of pulsed laser generated. Continuous-wave output beam from an 852nm ECDL is chopped into periodic laser pulses by a waveguide Mach-Zehnder-type electro-optic intensity modulator (MZ-EOIM).

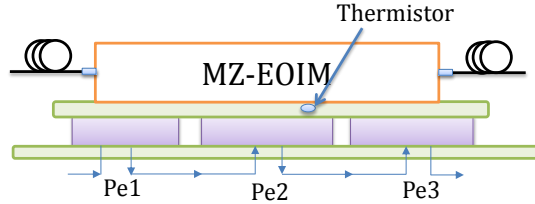


**Fig. 6.** (Color online) Diagrammatic drawing of temperature controlled system. Pe1, Pe2 and Pe3 in series are the Peltier modules, which are employed to heat or cool the EOIM. A thermistor connected to the temperature controller (not shown in this figure) is used to monitor and feedback the EOIM's temperature value.

In general,  $\text{LiNbO}_3$  waveguide with different crystal cut ways (X-cut, Y-cut, and Z-cut) is fabricated in wafers [16]. The Z-cut mode ridge waveguides increase the overlap between the applied electric field and the laser mode, which provides a lower half-wave voltage, but presents pyroelectric and thermo-optic effects. Because of the electrodes are directly located above the waveguide, the MZ-EOIM working condition is strongly affected by temperature. Due to the above-mentioned reasons, the DC bias voltage of the Z-cut MZ-EOIM used in our experiment drifts with the ambient temperature, which is problematic for generation of high on/off ratio laser pulses.

To suppress the DC bias voltage drifting caused by temperature change, we designed a temperature control device, as shown in Fig. 6. The MZ-EOIM package is placed on a thin copper plate with thermal grease to improve heating conduction. A  $10\text{ k}\Omega$  calibrated thermistor is placed inside copper plate for monitoring the MZ-EOIM's temperature. Install three parallel Peltier modules (thermal electric coolers, TECs) under the copper plate and connected with a temperature controller (Thorlabs, Model TED-200C) to stabilize the temperature. Typical temperature instability is less than 5 mK. The temperature-controlled MZ-EOIM is covered with an organic glass box to isolate it from the flow air and weaken temperature fluctuation.

#### IV. RESULTS AND DISCUSSIONS

As described by Eq. (4), we can trace the intensity at the outlet of the MZ-EOIM depending on the applied voltage, as shown in Fig. 7(a). The three curves represent different temperatures (296.4 K, 298.3 K, and 299.8 K). The maximum output power at the ON state is 7.5 mW. However, the minimum output power at the OFF state varies with the DC bias voltage, the incident polarization, and the MZ-EOIM's temperature. If the incident polarization is stable, power transmission curves at different temperatures will shift in specific direction. In principle, if there is no applied electronic signal (0 V), the relative phase shift between the two arms of the MZ-EOIM should be 0, and this yields that the transmitted power reaches maximum value. In Fig. 7(a), with no DC bias voltage (the vertical solid line), the temperature difference is less than 3.5 K, but output power varies seriously, corresponding to transmissivity varying from 99.6% to 45.8%, where the phase shift is caused by temperature due to the imbalance of two arm, pyroelectric effects[15] and temperature gradient between two arms[13]. Moreover, residual drift of the DC bias voltage at OFF state also indirectly changes output peak power. It is unacceptable that the Rabi frequency of excitation laser pulse varies over time in the triggered single-photon source [17]. Actually the power fluctuations at the OFF state will increase the probability of multiple excitations in one pulse period.

The phase shift depended on temperature is shown in Fig. 7(b), the temperature induced phase shift are about  $\pi/5.68$  K and  $\pi/5.58$  K , corresponding to DC bias voltage of 0V and 3V, respectively. This result may be viewed as a consequence of different arm length in MZ-EOIM or by considering that different thermal expansion induced by temperature gradient. The temperature-dependent extraordinary index of refraction in  $\text{LiNbO}_3$  was described by the below Sellmeier equation [19] :

$$n^2 = 5.35583 + 4.629 \times 10^{-7} f + \frac{0.100473 + 3.862 \times 10^{-8} f}{\lambda^2 - (0.20692 - 0.89 \times 10^{-8} f)^2} + \frac{100 + 2.652 \times 10^{-5} f}{\lambda^2 - 11.34927^2} - 1.5334 \times 10^{-2} \lambda \quad (6)$$

Where  $T_0 = 297.65$  K,  $\lambda = 0.852$   $\mu\text{m}$ , the temperature parameter  $f = (T - T_0)(T + T_0 + 2 \times 273.15)$  , the phase change  $\Delta\phi$  of the MZ-EOIM is generated by the voltage V applied to the electrodes:

$$\Delta\phi = k(\Delta n \cdot L_{DC} + n \cdot \Delta L) = (n^3 \gamma_{\text{eff}} V L_{DC} \lambda \pi / d + n k \Delta L) + \phi_0, \quad (7)$$

Where  $k = 2\pi/\lambda$  is the wavenumber of the incident beam, the effective electro-optic coefficient  $\gamma_{\text{eff}} = 30.8$  pm/V,  $L_{DC}$  is the DC electrode length,  $d$  is the distance of electrode,  $\Delta L$  and  $\phi_0$  represent the length difference and initial phase difference between two arms in waveguide, respectively. The open circle and square describe the DC voltage of 3V and 0V, respectively. The solid lines in Fig. 7(b) fit with Eq. (3) and (7), which shows a good agreement with the measured data in room temperature which is below 300 K. For temperature above 300K shown a little large deviation may be caused by temperature gradient between the sensor and the MZ-EOIM waveguide. The inset shown in Fig. 7(b) is the “double local minimum” of output power, so we choose the lowest local minimum as the OFF state to achieve a high on/off ratio. In fact the temperature induced phase shift includes asymmetric excitation and asymmetric arms [10, 19] and the pyroelectric field effects [20, 21], especially in the case of the different electrodes length [22].

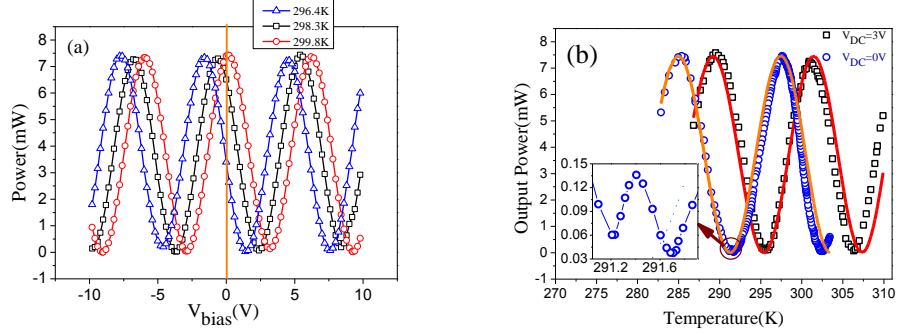


**Fig. 7.** (Color online) (a) The transfer function of the MZ-EOIM at three different temperatures which gives the dependence of the output laser power on the DC basis voltage. The blue triangles, the black squares, and the red circles represent the output laser power versus the DC bias voltage at temperature of 296.4 K, 298.3 K, and 299.8 K, respectively. (b) The transfer function of the MZ-EOIM at two different DC bias voltage of 3V and 0V, respectively, which gives the dependence of the output laser power on the temperature.

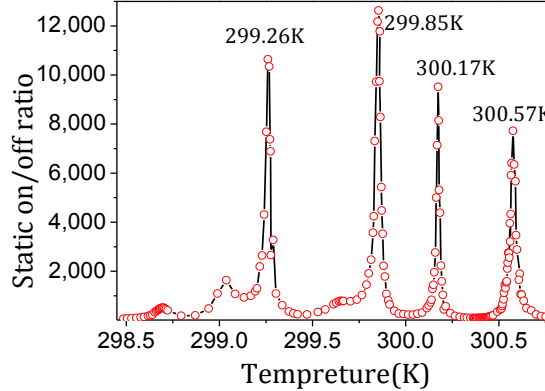


**Fig. 8.** (Color online) The measured static on/off ratio of MZ-EOIM at different temperature values.

After carefully matching the incident light polarization with the PM fiber and slowly changing the preset value of temperature controller, the OFF state can be searched at a specific bias voltage. If adding a half-wave voltage on the RF port, we can get the ON state. The measured static on/off ratios are shown in Fig. 8. The measured maximum on/off ratio is up to 12600:1, increasing by 21 dB compared with a typical value of 100:1. Every peak in Fig. 8 has a sharp slop, and they are similar to the expected curve profile in Fig. 4, corresponding to the symmetric of two arms tends to be perfect. One point should be addressed that the high on/off ratio can be achieved at low repetition rates, but at high repetition rates, such as megahertz, the on/off ratio will decrease, owing to power supply, the response speed of MZ-EOIM and the capacitance of coaxial cables. Finally, we measured the dynamic on/off in EOIM. The laser pulse trains, with duration of 5ns and various repetition rate from kilohertz to megahertz, were detected by Single Photon Counting modules (SPCM-AQRH-15-FC), and recorded by the P7888 card (FAST ComTec.). The acquisition card is triggered by the synchronized electrical pulse as the start. Then the dynamic on/off ratio can be shown in Fig. 9, in which the

dynamic on/off ratio is the ratio of the average photon counts per second in ON state and the average photon counts in OFF state per second. All measured the pulse trains was delivered into SPCM by multimode fiber after attenuate the output of the temperature-controlled MZ-EOIM. At a few kilohertz repetition rates, the on/off ratio remain above 5000, but gradually drop off to several hundred as the repetition rate is up to megahertz in Fig. 9(a), the same law can be seen when we increase the pulse duty ratio of 1MHz repetition rate in Fig. 9(b), which main is caused by the negative overshoot electronic signal and or the charge and discharge between electrodes. After the settling time of OFF state the residual photon counts similar to the static residual photon counts.

Due to the insertion loss of MZ-EOIM (including absorption), the input laser will heat the  $\text{LiNbO}_3$  waveguide. Also the applied electrical signal with certain power will cause heating. The temperature drift [20, 22] will change the refractive index, leading to phase shift fluctuation. When the phase difference of two arms fluctuates with the temperature, the DC bias voltage at the OFF state will change. Furthermore, the thermal effect will also cause the deformation of the waveguide geometry structure, leading to mismatching of the light mode inside the waveguide. It will affect the waveguide structure transmissivity of the arms ( $T_1$  and  $T_2$ ). As a result, it make beam splitting ratio of Y type deviate from 50/50. The temperature stabilization system can accurately match the temperature to optimum working point, at which the co-efficient balance between the two branches, thus the on/off ratio can increase remarkably.

In this method, because the peak intensity fluctuation percentage is much smaller than the OFF state, the power stability at OFF state directly reflects the stability of on/off ratio. As shown in Fig. 10, the MZ-EOIM not only reach a lower power at OFF state, but also the power drift can be remarkable suppressed. At the OFF state, the power drift of MZ-EOIM with temperature stabilization and without temperature stabilization are  $0.42\mu\text{W}/\text{h}$  and  $6.35\mu\text{W}/\text{h}$ , respectively. Generally, if we carefully match the temperature to make the temperature of MZ-EOIM waveguide reach a steady thermal equilibrium, which including Peltier modules, the internal laser power dispersion and RF electrical signal.

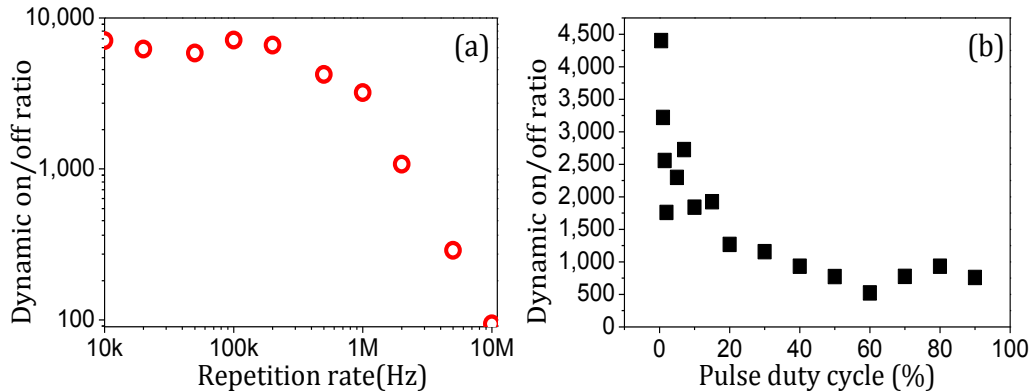


**Fig.9.** (Color online) (a) the dynamic on/off ratio of 5ns pulse duration versus laser pulse repetition rate, (b) the dynamic on/off ratio versus laser pulse duty cycle at repetition rate of 1MHz.

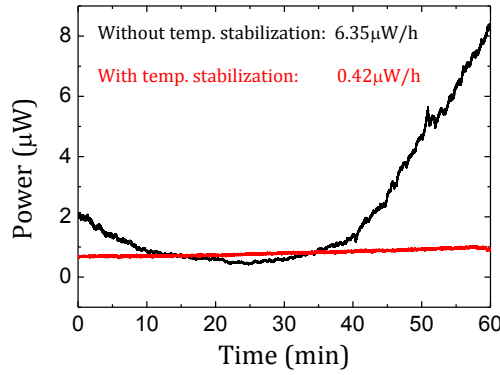


**Fig. 10.** (Color online) The power stability at OFF state in an hour, including with temperature stabilization (red solid line) and without temperature stabilization (black solid line).

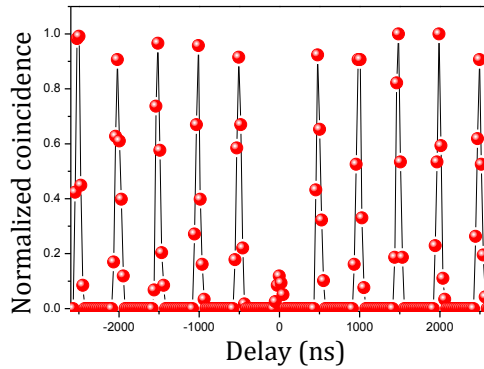


**Fig. 11.** (Color online) Anti-bunching of a triggered single-photon source based on trapped single cesium atom.

To prove the practicability of the high on/off ratio pulse laser, we have demonstrated the second-order intensity correlations of light field spontaneously emitted from the trapped single cesium atom, which is excited by 5ns pulse chain with a repetition rate of 2MHz. As shown in Fig.11, the results are measured by a Hanbury-Brown-Twiss setup [23] without any background subtraction, the coincidence close to zero around zero delay is the signature of a triggered single photon source.

## V. CONCLUSIONS

In conclusions, we have reanalyzed the model of transmitted light intensity of MZ-EOIM and found that the impact factors of the MZ-EOIM's on/off ratio are different transmittance of two arms ( $T_1 \neq T_2$ ), asymmetric splitting ratio, and combination ratio of Y-type structure. In addition the thermal fluctuation caused by heat exchange between the MZ-EOIM and thermal bath of laboratory environment, in fact, the MZ-EOIM also absorbs part of continuous-wave laser radiation and

electronic signals. In order to reduce heat accumulation, the temperature stabilization is implemented. We investigated the relationship between temperature and transmittance of MZ-EOIM, then concluded that temperature fluctuations seriously affect symmetric performance of the modulator, and further deteriorate the on/off ratio. In spite of this, choosing proper value by adjusting temperature, the symmetry of MZ-EOIM can be optimized to a near perfect point, and the static on/off ratio can be increased by at least 21 dB. The off state power drift is  $0.42\mu\text{W}$  in an hour, we can keep the on/off ratio of MZ-EOIM at a high value during several hours, but failed in several days, because of the finite temperature stability of laboratory environment. Further improvement requires recalibrating the temperature in time and designing a better temperature controlling system.

This system provides an elegant solution to the excitation laser pulses for the triggered single-photon source based on single atom manipulation, as well as a high signal-to-noise time-bin entanglement [24]. The single photon directly from single atoms may be more easy to enhance the atom-photon interaction in atomic ensemble and act as a quantum memory due to narrow bandwidths (about 5 MHz) [25]. The proposed technique is suitable for general asymmetric MZ-EOIM, and the analysis and discussion may provide some references for MZ-EOIM manufacture to accelerate the development of the quantum information process.

## ACKNOWLEDGMENTS

This project is supported by the National Natural Science Foundation of China (Grant Nos. 11274213, 61475091, 61205215, and 61227902), and the National Major Scientific Research Program of China (Grant No. 2012CB921601).

## References

- [1] E. L. Wooten, K. M. Kiss, A. Yi-Yan, E. J. Murphy, D. A. Lafaw, P. F. Hallemeier, D. Maack, D. V. Attanasio, D. J. Fritz, G. J. McBrien, and D. E. Bossi, *IEEE J. Sel. Top. Quant. Electron.* **6**, 69-82 (2000).
- [2] T. Kawanishi, T. Sakamoto, and M. Izutsu, *IEEE J. Sel. Top. Quant. Electron.* **13**, 79-91 (2007).
- [3] B. Darquié, M. P. A. Jones, J. Dingjan, J. Beugnon, S. Bergamini, Y. Sortais, G. Messin, A. Browaeys, and P. Grangier, *Science* **309**, 454-456 (2005).
- [4] S. Garcia, D. Maxein, L. Hohmann, J. Reichel, and R. Long, *Appl. Phys. Lett.* **103**, 114103 (2013).
- [5] J. Dingjan, B. Darquié, J. Beugnon, M. P. A. Jones, S. Bergamini, G. Messin, A. Browaeys, and P. Grangier, *Appl. Phys. B* **82**, 47-51 (2006).
- [6] H. Nagata, S. Oikawa and M. Yamada, *Opt. Eng.* **36**, 283-286 (1997).
- [7] J. He, B. D. Yang, Y. J. Cheng, T. C. Zhang, and J. M. Wang, *Front. Phys.* **6**, 262-270 (2011).
- [8] L. Terlevich, S. Balsamo, S. Pensa, M. Pirola, and G. Ghione, *J. Lightwave Technol.* **24**, 2355-2361 (2006).
- [9] N. Grossard, J. Hauden, and H. Porte, US Patent WO2006/129035S.
- [10] J. Snoddy, L. Yun, F. Ravet, and X. Y. Bao, *Appl. Opt.* **46**, 1482-1485 (2007).
- [11] D. T. Bui, C. T. Nguyen, I. Ledoux-Rak, J. Zyss, and B. Journet, *Meas. Sci. Technol.* **22**, 125105 (2011).

- [12] X. Y. Wang, J. Q. Liu, X. F. Li, and Y. M. Li, IEEE J. Quant. Electron. **51**, 5200206 (2015).
- [13] J. P. Salvestrini, L. Guilbert, M. Fontana, M. Abarkan, and S. Gille, J. Lightwave Technol. **29**, 1522-1534 (2011).
- [14] K. Suzuki, T. Yamada, and O. Moriwaki, IEEE Photon. Technol. Lett. **20**, 773-775 (2008).
- [15] R. S. Weis and T. K. Gaylord, Appl. Phys. A **37**, 191-203 (1985).
- [16] M. L. Harris, C. S. Adams, S. L. Cornish, I. C. McLeod, E. Tarleton, and I. G. Hughes, Phys. Rev. A **73**, 062509 (2006).
- [17] D. Janner, D. Tulli, M. Belmonte, and V. Pruneri, J. Opt. A: Pure Appl. Opt. **10**, 104003 (2008).
- [18] H. J. Metcalf and P. van der Straten, *Laser Cooling and Trapping* (Springer, 1999).
- [19] H. Nagata, N. F. O’Beirn, W. R. Bosenberg, G. L. Reiff, and K. R. Voisine, IEEE Photon. Technol. Lett. **16**, 2460-2462 (2004).
- [20] D. H. Jundt, Opt. Lett. **20**, 1553-1555 (1997).
- [21] H. Nagata and K. Kiuchi, J. Appl. Phys. **73**, 4162–4164 (1993).
- [22] P. Skeath, C. H. Bulmer, S. C. Hiser, and W. K. Burns, “Novel electrostatic mechanism in the thermal instability of z-cut LiNbO<sub>3</sub> interferometers,” Appl. Phys. Lett. **49**, 1221-1223 (1986).
- [23] R. Hanbury Brown and R. Q. Twiss, Nature **177**, 27 (1956).
- [24] T. Inagaki, N. Matsuda, O. Tadanaga, M. Asobe, and H. Takesue, Opt. Express **21**, 23241 (2013).
- [25] K. S. Choi1, H. Deng, J. Laurat, and H. J. Kimble, Narure **452**, 67 (2008).